VLA Test Memo 143

R. Sramek

October 20, 1983

"VLA Phase Stability at 22 GHz on Baselines of 100m to 3km"

## 1.     Introduction:

Reports from observers tell us that the K band phase stability ranges from very good to hopelessly bad and is often some where in between. This is not very helpful for engineering purposes.  Here I will try to make some more quantitative statements about the VLA phase stability based on a series of ten test observing runs at 22 GHz made between 82 Nov and 83 July.  This study deliniates the range of expected phase stability and offers some hope that the VLA site may be useful at wavelengths shorter than 1.3cm.

## 2.     Fundamentals:

Consider the visibility phases of an unresolved radio source, measured on a particular baseline, as a time series.  The properties of this time series depend on several parameters that we use to restrict the data. Some of the more important parameters are given below.

$T_{ave}$     is the averaging time of the individual phase points.  This sets the high frequency cutoff of the power spectrum of the time series.

$T_{sam}$     is the sampling period of the time series.

$T_{max}$     is the longest period observable in the time series, e.g., this may correspond to the length of the observation.

B     is the baseline length, i.e., the separation between the antennas; this determines the longest spatial component of the atmosphereic phase distortion that contributes to the time series.

$\Delta(\alpha,\delta)$ is the angular separation in the sky between the radio source and any observed calibrator phase that is subtracted from the time series.

$T_{cal}$ is the characteristic time scale of the calibration.

In addition, the calibration time series may have its own $T_{ave}$ and $T_{sam}$. The $T_{cal}$ will be determined by the type of interpolation used for the calibration ( two-point, boxcar, etc.).

These parameters must be specified whenever we try to compare phase stabilities determined by various observers.

In addition there are many physical characteristics of the atmosphere at the time of observations that determine the phase stability. Since we hope to eventually link the observed phase stability with atmospheric parameters, information such as atmospheric water vapor content, wind velocity, atmospheric lapse rate, barometric pressure, etc. should be given if possible.

## 2.1     The Allan Variance

The visibility phase time series can be completely characterized by its power spectrum. Howerver, there are serveral disadvantages with using this technique. First, the interferometer phases show a low frequency divergence, or at least the power in the time series is heavily dominated by the longest period sampled. The amplitude of these very long periods, and the amplitude of the sidebands splattered into the higher frequencies, are largely determined by the type of high pass filtering, if any, that the person doing the analysis decides to use. Also, the power spectrum gives too much information about the time series; all we want are a few numbers that chacterize the phase stability which we can correlate with the atmospheric parameters.

In the study of oscillator phase and frequency stability, an Allan variance analysis is often used to circumvent these problems (Blair 1974, Kartaschoff 1978). The Allan variance has a well defined relationship to the phase power spectrum and the phase structure function. It also can be linked to the three-dimensional spatial power spectrum of the atmospheric refractive index (Armstrong and Sramek, 1982, and references cited therin). For a given sampling period, the Allan variance is not very dependent on the total length of the observation or the number of samples. Also, in the limiting case of the two sample variance, this function it is very easy to calculate.

$\Delta(\alpha,\delta)$  is the angular separation in the sky between the radio source and any observed calibrator phase that is subtracted from the time series.

$T_{cal}$  is the characteristic time scale of the calibration.

In addition, the calibration time series may have its own $T_{ave}$ and $T_{sam}$. The $T_{cal}$ will be determined by the type of interpolation used for the calibration ( two-point, boxcar, etc.).

These parameters must be specified whenever we try to compare phase stabilities determined by various observers.

In addition there are many physical characteristics of the atmosphere at the time of observations that determine the phase stability.  Since we hope to eventually link the observed phase stability with atmospheric parameters, information such as atmospheric water vapor content, wind velocity, atmospheric lapse rate, barometric pressure, etc. should be given if possible.

## 2.1    The Allan Variance

The visibility phase time series can be completely characterized by its power spectrum.  Howerver, there are serveral disadvantages with using this technique.  First, the interferometer phases show a low frequency divergence, or at least the power in the time series is heavily dominated by the longest period sampled.  The amplitude of these very long periods, and the amplitude of the sidebands splattered into the higher frequencies, are largely determined by the type of high pass filtering, if any, that the person doing the analysis decides to use. Also, the power spectrum gives too much information about the time series; all we want are a few numbers that chacterize the phase stability which we can correlate with the atmospheric parameters.

In the study of oscillator phase and frequency stability, an Allan variance analysis is often used to circumvent these problems (Blair 1974, Kartaschoff 1978).  The Allan variance has a well defined relationship to the phase power spectrum and the phase structure function.  It also can be linked to the three-dimensional spatial power spectrum of the atmospheric refractive index (Armstrong and Sramek, 1982, and references cited therin).  For a given sampling period, the Allan variance is not very dependent on the total length of the observation or the number of samples.  Also, in the limiting case of the two sample variance, this function it is very easy to calculate.

The fractional frequency stability, y(t), is given by

$$y(t) = \delta f(t) / f_o \qquad (1)$$

where $\delta f(t)$ is the deviation at time t of the oscillator frequency from a mean frequency $f_o$. The two sample Allan variance with zero dead time between frequency measurements is defined as

$$\sigma_y^2(T) = \tfrac{1}{2} \left\langle \left( y_{i+1}(T) - y_i(T) \right)^2 \right\rangle_i. \qquad (2)$$

where T is the time over which the fractional frequency observation is made. Writing this in terms of phase,

$$\sigma_y^2(T) = \frac{1}{2} \frac{1}{N} \sum_{i=1}^{N} \left[ \frac{(\phi_{i+2} - \phi_{i+1})}{Tf_o} - \frac{(\phi_{i+1} - \phi_i)}{Tf_o} \right]^2 \qquad (3)$$

$$\tfrac{1}{2} f_o^2 T^2 \sigma_y^2(T) = \frac{1}{N} \sum_{i=1}^{N} \left[ \frac{\phi_{i+2} - \phi_i}{2} - \phi_{i+1} \right]^2 \qquad (4)$$

$$\frac{1}{\sqrt{2}} f_o T \sigma_y(T) = \sigma_A(T) \qquad (5)$$

Thus, the rms of the phase after a two-point calibration (denoted by $\sigma_A(T_{sam})$ ) is just $1/\sqrt{2}$ times the two point Allan variance expressed as a phase. Here the source-calibrator cycle time $T_{cal} = 2*T_{sam}$, and the source calibrator separation is $\Delta(\alpha, \delta) = 0$.

In addition to $\sigma_A(T_{sam})$ derived from the Allan variance, for comparison I've calculated the rms phase (denoted by $\sigma_B$) for each time series after first removing a phase drift in time. If this linear phase drift were not removed, the rms values would reflect baseline, UT1, and source position errors in addition to the atmospheric and instrumental drifts that we would like to measure.

3. THE DATA

The ten K-band test observing runs are described in Table I. Typically, each run lasted 4 hours and consisted of 8 minute scans alternating between two sources. The source elevations were typically 40 to 30 degrees. Two pairs of sources were used. On five days the separation of

3

the sources was 23 degrees, and on 4 days the source separation was 6 degrees. These eight minute scan averages were the primary data sets that were analysed. Parts of the November and June observations and the entire March run consisted of long scans on a single source to study the Allan variance as a function of $T_{sam}$.

A reference antenna was picked for each observing run that gave a variety of baseline lengths to the other antennas. Typically, twenty to twenty-four antenna pairs were used in the analysis. All the data was taken in either the C or the D configurations, giving baselines of length 60 to 3000m. Since the phase errors are largely antenna based, there is little additional information to be had by considering all possible antenna pairs.

The Allan variance of the phase was calculated for each observing run, for each source on each baseline. Also, the Allan variance was calculated for the difference in phase between the two sources using the normal two point calibration used at the VLA. These Allan variances, expressed as $\sigma_A$ in degrees of phase at 1.3 cm wavelength, were plotted as a function of baseline length. Fig. 1-3 show typical log-log the plots of $\sigma_A$ for days with very good, average, and poor phase stability.

The $\sigma_A$ follow a power law with

$$\sigma_A(T_{sam},B) = \sigma_{A:1km}(T_{sam}) * B^{\alpha} .$$

The slope of the power law, $\alpha$, and the 1km intercept, $\sigma_{A:1km}$, will be used to characterize the phase stability of each day. The least square fit of this power law is shown on each plot.

In a similar manner, the slope and 1km intercept of $\sigma_B$ was calculated for each observing run.

4. RESULTS

4.1 Allan Variance Analysis

Table II gives the slope and 1km intercept of $\sigma_A(T_{sam}=16min,B)$ for each of the ten days. Here $T_{ave} = 8min$. The average values are given at the bottom of the table.

The slope and intercept are also given for the difference in phase of the two sources, i.e., the calibrated phase. Since $\sigma_A$ is like a self-calibration with $\Delta(\alpha,\delta) = 0$ and $T_{cal} = 2*T_{sam} = 4*T_{ave}$, the additional calibration on the second source with $T_{cal} = T_{sam}$ is not expected to lower the $\sigma_A$ very much. The observed mean phase of the 1km intercept is only reduced from 18 degrees to 16 degrees by calibration.

the sources was 23 degrees, and on 4 days the source separation was 6 degrees. These eight minute scan averages were the primary data sets that were analysed. Parts of the November and June observations and the entire March run consisted of long scans on a single source to study the Allan variance as a function of $T_{sam}$.

A reference antenna was picked for each observing run that gave a variety of baseline lengths to the other antennas. Typically, twenty to twenty-four antenna pairs were used in the analysis. All the data was taken in either the C or the D configurations, giving baselines of length 60 to 3000m. Since the phase errors are largely antenna based, there is little additional information to be had by considering all possible antenna pairs.

The Allan variance of the phase was calculated for each observing run, for each source on each baseline. Also, the Allan variance was calculated for the difference in phase between the two sources using the normal two point calibration used at the VLA. These Allan variances, expressed as $\sigma_A$ in degrees of phase at 1.3 cm wavelength, were plotted as a function of baseline length. Fig. 1-3 show typical log-log the plots of $\sigma_A$ for days with very good, average, and poor phase stability.

The $\sigma_A$ follow a power law with

$$\sigma_A(T_{sam},B) = \sigma_{A:1km}(T_{sam}) * B^{\alpha} .$$

The slope of the power law, $\alpha$, and the 1km intercept, $\sigma_{A:1km}$, will be used to characterize the phase stability of each day. The least square fit of this power law is shown on each plot.

In a similar manner, the slope and 1km intercept of $\sigma_B$ was calculated for each observing run.

4. RESULTS

4.1 Allan Variance Analysis

Table II gives the slope and 1km intercept of $\sigma_A(T_{sam}=16min,B)$ for each of the ten days. Here $T_{ave} = 8min$. The average values are given at the bottom of the table.

The slope and intercept are also given for the difference in phase of the two sources, i.e., the calibrated phase. Since $\sigma_A$ is like a self-calibration with $\Delta(\alpha,\delta) = 0$ and $T_{cal} = 2*T_{sam} = 4*T_{ave}$, the additional calibration on the second source with $T_{cal} = T_{sam}$ is not expected to lower the $\sigma_A$ very much. The observed mean phase of the 1km intercept is only reduced from 18 degrees to 16 degrees by calibration.

## 4.2 RMS about a Linear Phase Drift

Table III gives the slope and 1km intercept for $\sigma_B$, the RMS about a linear phase drift in time. $T_{ave}$ is 8 minutes. For the uncalibrated data $T_{cal}$ is effectively about 4 hours and $\Delta(\alpha,\delta) = 0$. Phase drifts with periods of 8 minutes to 4 hours exist in the time series and therefore $\sigma_B$ is somewhat larger than $\sigma_A$. When the two point calibration is applied $T_{cal}$ is 16 minutes.

The effect of calibration is shown in Figure 4. The 1km intercept of the calibrated and uncalibrated phases are shown separately for the two pairs of sources with $\Delta(\alpha,\delta) = 6$ degrees and 23 degrees. In general, the calibration only slightly improves the phase r.m.s. and this improvement is not a strong function of angular separation in the 6 to 23 degree range. The average $\sigma_{B:1km}$ is only reduced by 3 degrees when calibration is applied.

## 4.3 Separating the Instrumental and Atmospheric Phase Errors

Both the instrument and the troposphere contribute to the observed phase errors (the ionospheric contribution is negligible at 1.3cm). The errors due to the troposphere and some of the instrumental contribution are the same in both polarization channels. However, part of the instrumental phase error (e.g. that due to receiver noise) is uncorrelated in the two polarizations and can be estimated by differencing the phases in the two channels. This part of the error is observed to be typically 2 degrees for $T_{ave} = 8$min. It is rather independent of $T_{sam}$ and is about the same for $\sigma_A$ and $\sigma_B$. Since this instrumental error is much smaller than most of our observed total phase errors, no correction has been applied.

This 2 degree error represents the minimum instrumental contribution. In addition, there is certainly an LO phase error which is not reflected in the phase difference test. This error may increase with baseline length although we don't have a well defined mechanism to produce such an effect.

Therefore, the observed phase errors discussed here represent a total system phase and are an upper limit to the atmospheric contribution. This is encouraging since instruments can conceivably be improved but the atmosphere can't (however, we may be able to monitor it better).

## 4.4 Average Phase Stability

In order to make some general statement about phase stability, the $\sigma_A$ measured on all days, on all baselines, and for all sources were binned according to baseline length and averaged. The same was done for the $\sigma_B$. The results are summarized in Table IV. Figures 5 and 6 show these

average results for the uncalibrated $\sigma_A$ with $T_{sam}$ = 16min and 32min. Figure 7 shows the average result for the calibrated $\sigma_B$. Since each binned data point represents about 30 observations on ten independent days, the dispersion of the values within each bin can be used to show the range of expected phase stability. The dotted lines represent the least square fit power law to the points one standard deviation above and below the mean line. In general, observations at the VLA have a 68% chance of having an rms phase lieing within the dotted lines.

The results in Table IV show that the 1km intercept is typically 17 degrees and has little dependence on the $T_{sam}$ between 16 min and 32 min. It is not greatly effected by calibration, and is quite independent of the manner of analysis.

5. The Allan Variance as a Function of $T_{sam}$.

$\sigma_A$ gives the phase stability on time scale $T_{sam}$. The total rms phase is equal to

$$\sigma = \left[ \sigma_A^2(T_{sam}) + \sigma_A^2(2*T_{sam}) + \sigma_A^2(4*T_{sam}) + (et\ cet.) \right]^{\frac{1}{2}}$$

up to $2*T_{sam} = T_{max}$ (Rogers and Moran, 1981). $T_{max}$ is determined by the duration of the observation or by the time scale on which the cross correlation of the phase errors of the source and calibrator falls to zero. This latter time scale probably increases as the source-calibrator separation increases.

The long observing run on March 26 gives a good analysis of the dependence of $\sigma_A$ as a function of $T_{sam}$ and $T_{ave}$. The $\sigma_A$(B=1km, $T_{sam}$) shown in Figure 8 is fairly flat from $T_{sam}$ = 1 minute to 4 minutes and corresponds to white phase noise. From $T_{sam}$ = 4 minutes to 32 minutes the phase goes as $T_{sam}^{.27}$, slightly steeper than flicker phase noise which goes appproximately as $T_{sam}^{.15}$.

This figure is useful for combining dispersions calculated with different averaging times or sampling times. Based on limited data, the white phase noise and the failure of the noise to reduce as $T_{ave}^{-.5}$ are characteristic of the atmospheric fluctuations for baselines less than a couple kilometers.

6. Phase Stability and Observing Conditions

The on line computers at the VLA apply an atmospheric phase correction based on the surface barometric pressure, temperature, and water vapor content (dew point). These corrections are based on an atmospheric model and they remove the large scale effects of the troposphere. The observed

residual phases reflect the failure of the model, probably on small (ten degree) angular scales.

The parameter $\sigma_{A:1km}$ offers a good measure of the phase stability on a given day. Using $T_{sam}$ = 16 minutes and $T_{ave}$ = 8 minutes as reasonable observing parameters, I've taken the uncalibrated $\sigma_{A:1km}$ shown in Table II, averaged the data for the pair of sources, and compared this quantity with the time/day, the index of refraction due to water vapor, and the wind velocity (Figures 9, 10, and 11 respectively).

Figure 9 indicates that afternoons have poorer phase stability than the rest of the day. Four out of the five runs where $\sigma_{A:1km}$ is greater than 15 degrees occur between 1200 and 1800 MST.

Figure 10 shows no great correlation between water vapor measured at the ground level and the residual phase errors. Either the surface measurements don't reflect the small scale upper atmosphere water vapor content, or water vapor is not the major source of phase error (e.g. we're seeing phase errors due to the dry air contribiution), or the stability of the troposphere is more important than the amount of water vapor.

Figure 11 shows some tendency for the greater phase errors to occur on days with higher wind velocity. Two possible explanations come to mind. First, the phase errors may be due to mechanical motion of the antennas on windy days. Noting that the phase errors get worse on longer baselines, this implies that wind driven antenna movements are the same over a few hundred meters, but at progressivly longer baselines the winds decorrelate and the resulting antenna movements produce baseline errors and thus phase errors. Antenna movements of about a millimeter would explain this effect. The second possible explanation is that wind induced turbulence (in either the wet or the dry air component or both) is causing the observed phase errors. A search for detailed correlation between the wind velocity vector at two antennas (or the antenna tilt) and the phase error could test the first hypothesis.

7. Phase Stability at Shorter Wavelengths

Using $T_{sam}$ = 16 min as typical of a calibrated observing run, Figure 5 allows us to predict how an array of various sizes will perform at shorter wavelength. If you accept one radian as the upper limit of acceptable phase stability for an interferometer, the 14 degree line at 22 GHz in Figuer 5 corresponds to a radian at 88 GHz. For half the time, an array 1 km in size will have phase stability better than this. Longer baselines will have fewer days of acceptable stability.

The phase stability shown in Figure 5 represent the total system phase and is not necessarily a limit impossed by the atmosphere. To the extent

7

that the phase errors are due to l.o. phase instability or mechanical motion of the antennas the phase stability can conceivably be improved.

Even if the phase errors arise in the atmosphere, water vapor radiometers may give a useful phase correction. And finally, we may be able to predict the time of day or year which give the best phase stability and schedule the shortest wavelength and longest baseline observations at this time.


8. Conclusions

a) The best estimate for the average uncalibrated rms phase, with a time scale of 16 minutes and baselines from 100m to 3000m, is approximately

$$\sigma = (16 \pm 3) \; B(km)^{0.36} \quad degrees$$

This represents an average of $\sigma_A$ uncalibrated and $\sigma_B$ calibrated. The result does not change much by varying the time scale by a factor of two.

b) Since the phase rms given in a) contains a contribution of unknown magnitude from l.o. instabilities, this is an upper limit to the atmospheric phase stability.

c) For baselines of order 1km, $\sigma_A$ is not a strong function of $T_{sam}$. Two time ranges are important. For $T_{sam}$ = 1 to 4 minutes we have white phase noise and the phase error is constant. From 4 to 32 minutes, we are in the flicker phase regime, where $\sigma_A = T_{sam}^{.27}$, giving a 20% increase of phase noise for each doubling of $T_{sam}$. The relevant time scales may change at longer baselines since we would be sampling different size scales in the troposphere.

d) For baselines of order of 1km, $T_{cal}$ = 16 minutes, and with source-calibrator separations of 6 degrees to 23 degrees, two-point calibration does little to improve the phase stability. An average improvement of only three degrees out of twenty can be expected, and this improvement is not a strong function of source-calibrator separation. Only with angular separations of less than a few degrees, where the source/calibrator phase fluctuations are correlated, will rapid switching ($T_{cal}$ ~ 8 minutes, see c) above) be of any help.

e) The phase stability is not worse on days with high dew point, but is worse on days with high wind velocity, usually in the afternoon. This may be due to wind induced turbulence in the atmosphere or to mechanical motion of the antennas.

f) Phase errors of less than one radian can be expected for half the time at baselines up to 1 kilometer at 3mm wavelength.

Blair, B.E., 1974, "Time and Frequency: Theory and Fundamentals", National Bureau of Standards Monograph 140, U.S. Government Printing Office, Washington, D.C.

Kartaschoff, P., 1978, "Frequency and Time", Academic Press, New York, NY

Rogers, A.E. and Moran, J.M., 1981, I.E.E.E. Trans. on Instrumentation and Measurement, IM-30, 283.

## TABLE I

Summary of 22.5 GHz Phase Stability Test Observations

| Date | Time (MST) Start | Stop | Sources | Observation |
|------|-------|------|---------|-------------|
| 82nov13 | 0300 | 1010 | 0923+392 0917+624 | alternate 8min scan; 2.5hr plus single 2.7hr scan |
| 82dec28 | 0145 | 0645 | 0923+392 0917+624 | alternate 8min scan; 4.9hr |
| 83jan13 | 2130 | 0130 | 0923+392 0917+624 | alternate 8min scan; 3.9hr |
| 83jan15 | 1330 | 1630 | 0224+671 0212+735 | alternate 8min scan; 2.9hr |
| 83feb21 | 0700 | 1300 | 0224+671 0212+735 | alternate 8min scan; 6.0hr |
| 83mar26 | 0300 | 0700 | 1803+784 | single scan; 3.9hr |
| 83apr11 | 1300 | 1700 | 0224+671 0212+735 | alternate 8min scan; 3.6hr |
| 83may27 | 0500 | 1000 | 0224+671 0212+735 | alternate 8min scan; 5.0hr |
| 83jun04 | 1220 | 1620 | 0923+392 0917+624 | alternate 8min scan; 4.0hr |
| 83jul02 | 1030 | 1430 | 0923+392 0917+624 | alternate 8min scan; 3.9hr |

TABLE II

Summary of results for $\sigma_A$ at 22.5 GHz

$T_{sam}$ = 16min

| Date | Source Declination (degrees) | NO CAL $\sigma/\alpha$ | $\sigma_{A:1km}$ (degrees) | CAL APPLY $\alpha$ | $\sigma_{A:1km}$ (degrees) |
|------|------|------|------|------|------|
| 82nov13 | 39 | .554 | 14.1 | .514 | 11.1 |
|  | 62 | .712 | 11.1 |  |  |
| 82dec28 | 39 | .619 | 7.6 | .604 | 7.8 |
|  | 62 | .301 | 8.4 |  |  |
| 83jan13 | 39 | .268 | 4.7 | .431 | 5.1 |
|  | 62 | .560 | 9.2 |  |  |
| 83jan15 | 73 | .576 | 21.7 | .449 | 18.4 |
|  | 67 | .801 | 17.5 |  |  |
| 83feb21 | 73 | .525 | 9.5 | .540 | 9.4 |
|  | 67 | .595 | 12.7 |  |  |
| 83mar26 | 78 | .726 | 21.6 |  |  |
| 83april1 | 73 | .810 | 32.0 | .782 | 34.2 |
|  | 67 | .741 | 28.9 |  |  |
| 83may27 | 73 | .619 | 9.0 | .612 | 9.3 |
|  | 67 | .647 | 10.1 |  |  |
| 83jun04 | 39 | .683 | 36.0 | .658 | 37.0 |
|  | 62 | .923 | 59.2 |  |  |
| 83jul02 | 39 | .349 | 9.8 | .327 | 10.5 |
|  | 62 | .611 | 24.2 |  |  |
| AVERAGE |  | <.612> | <18.3> | <.546> | <15.9> |

NOTE: rms phase(degrees @ 22.5 GHz) = $\sigma_{A:1km} * B^\alpha$

where B = baseline length in kilometers

TABLE III

Summary of results for $\sigma_B$ at 22.5 GHz

| Date | Source Declination (degrees) | NO CAL $\alpha$ | $\sigma_{B:1km}$ (degrees) | CAL APPLY $\alpha$ | $\sigma_{B:1km}$ (degrees) |
|------|------|------|------|------|------|
| 82nov13 | 39 | .274 | 18.8 | .454 | 10.8 |
|         | 62 | .346 | 18.8 |      |      |
| 82dec28 | 39 | .410 | 10.1 | .396 | 7.8 |
|         | 62 | .422 | 9.5 |      |      |
| 83jan13 | 39 | .302 | 16.2 | .512 | 10.1 |
|         | 62 | .363 | 14.5 |      |      |
| 83jan15 | 73 | .613 | 24.5 | .296 | 17.9 |
|         | 67 | .556 | 20.0 |      |      |
| 83feb21 | 73 | .241 | 22.6 | .534 | 14.7 |
|         | 67 | .222 | 23.5 |      |      |
| 83mar26 | 78 | .811 | 24.0 |      |      |
| 83apr11 | 73 | .788 | 34.4 | .866 | 42.6 |
|         | 67 | .689 | 29.7 |      |      |
| 83may27 | 73 | .269 | 16.8 | .669 | 12.1 |
|         | 67 | .323 | 18.5 |      |      |
| 83jun04 | 39 | .644 | 43.0 | .650 | 44.9 |
|         | 62 | .666 | 46.8 |      |      |
| 83jul02 | 39 | .421 | 18.3 | .456 | 17.1 |
|         | 62 | .587 | 26.4 |      |      |
| AVERAGE | | <.471> | <23.0> | <.537> | <19.8> |

NOTE: rms phase(degrees @ 22.5 GHz) = $\sigma_{B:1km} * B^{\alpha}$

where B = baseline length in kilometers

12

TABLE IV
Single Power Law Fit to All Data

| Type of Solution | NO CAL | | CAL APPLY | |
|---|---|---|---|---|
| | $\alpha$ | $\sigma_{.1km}$ (degrees) | $\alpha$ | $\sigma_{.1km}$ (degrees) |
| $\sigma_A$ ($T_{sam}$=16min) | .362 | 14.5 | .288 | 13.1 |
| $\sigma_A$ ($T_{sam}$=32min) | .410 | 17.3 | .337 | 16.4 |
| $\sigma_B$ | .375 | 21.5 | .351 | 17.2 |

p018a1; cal:none; alt sig2pt; rebin 0
tau = 16 min



$\phi = 36°$ $B_{km}$ .68

Log(m)

Log($\frac{dog}{sd}$) phase

F 3. 1

p018a1; cal:none; alt sig2pt; rebin 0
tau = 16 min

Log(m)

Log($\frac{deg}{cpd}$) phase

$\phi = 36°$  B$_{km}$ .68
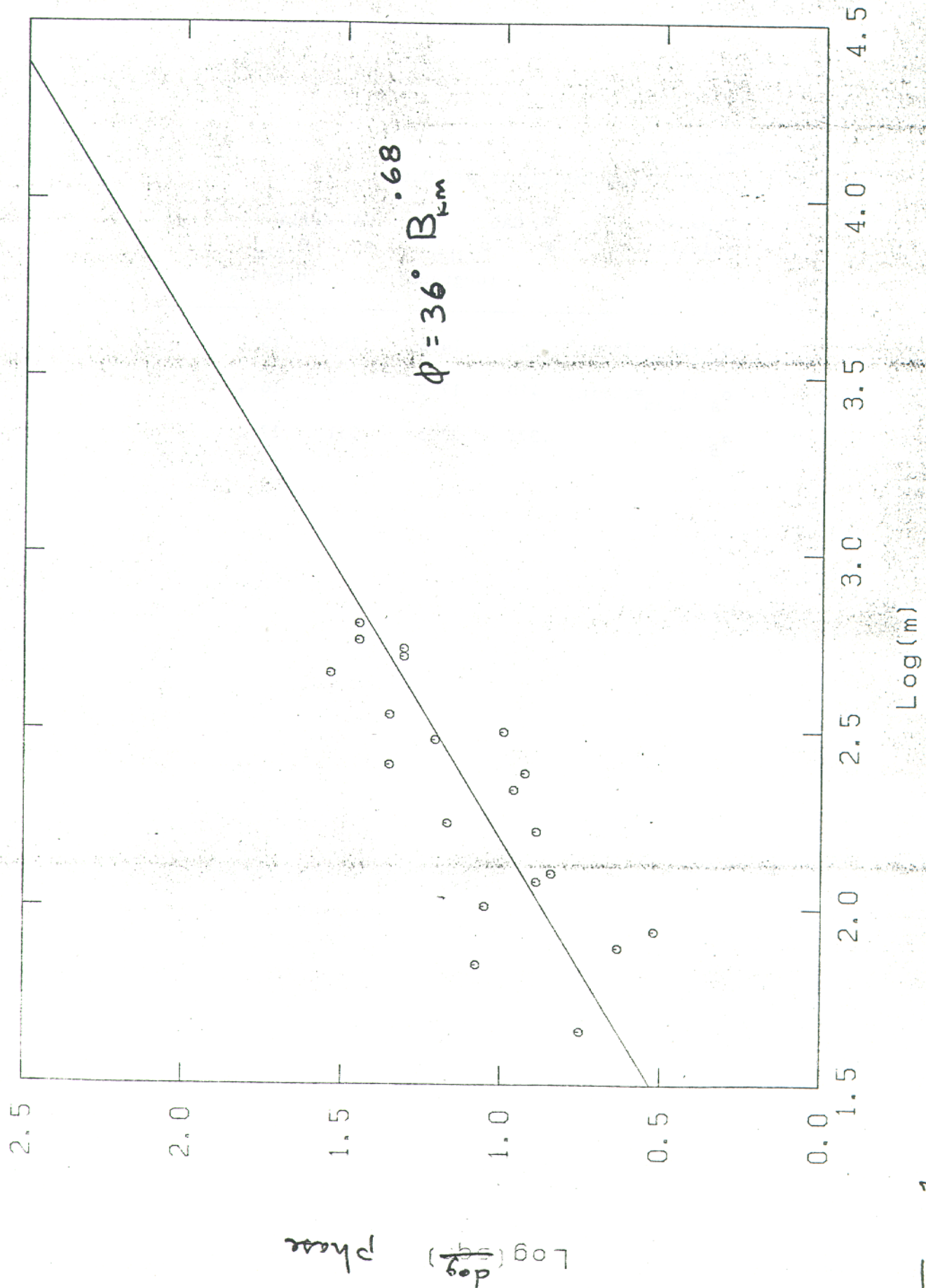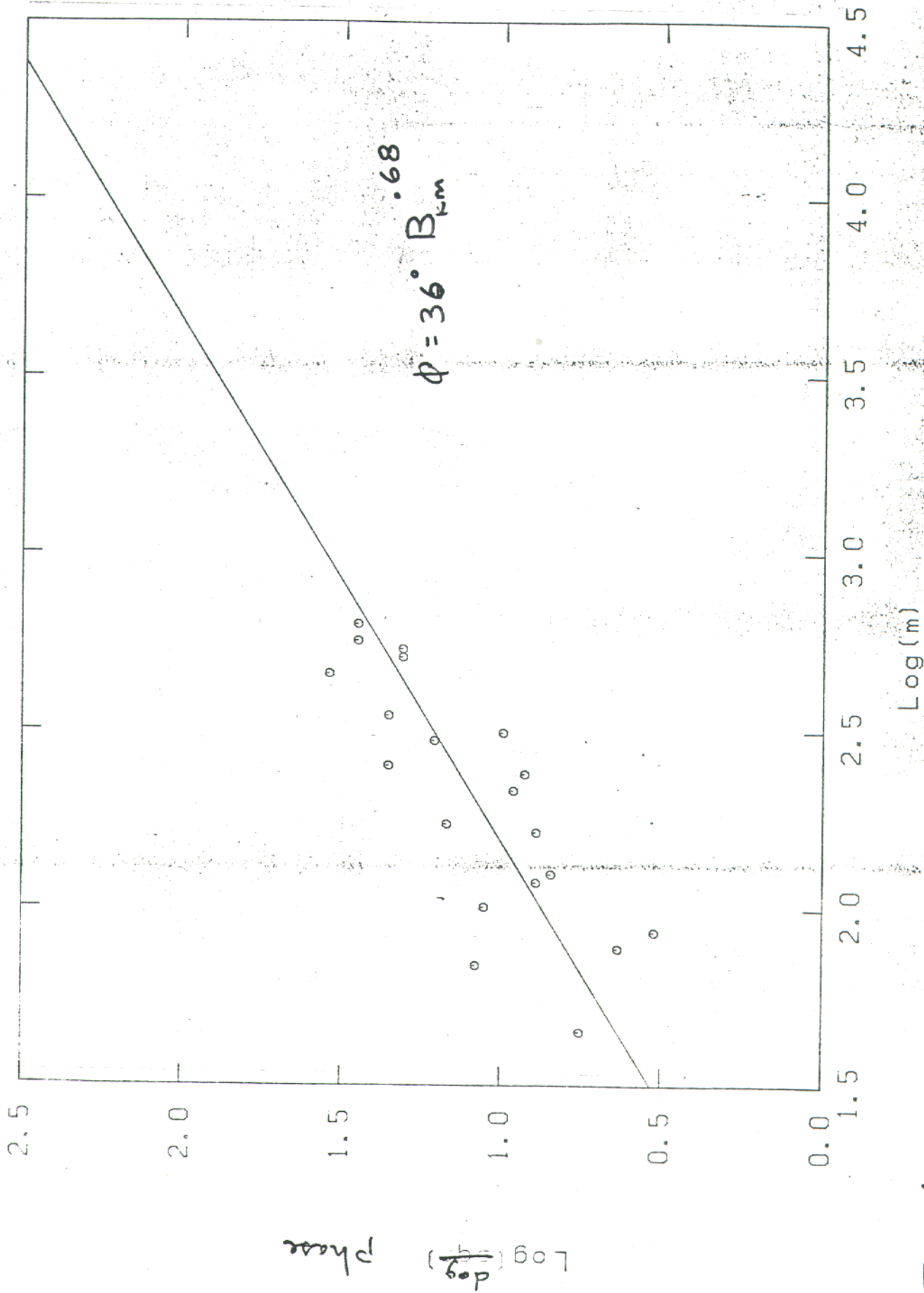
Fig. 1

p017a1; cal:none; alt sig2pt; rebin 0
tau = 16 min
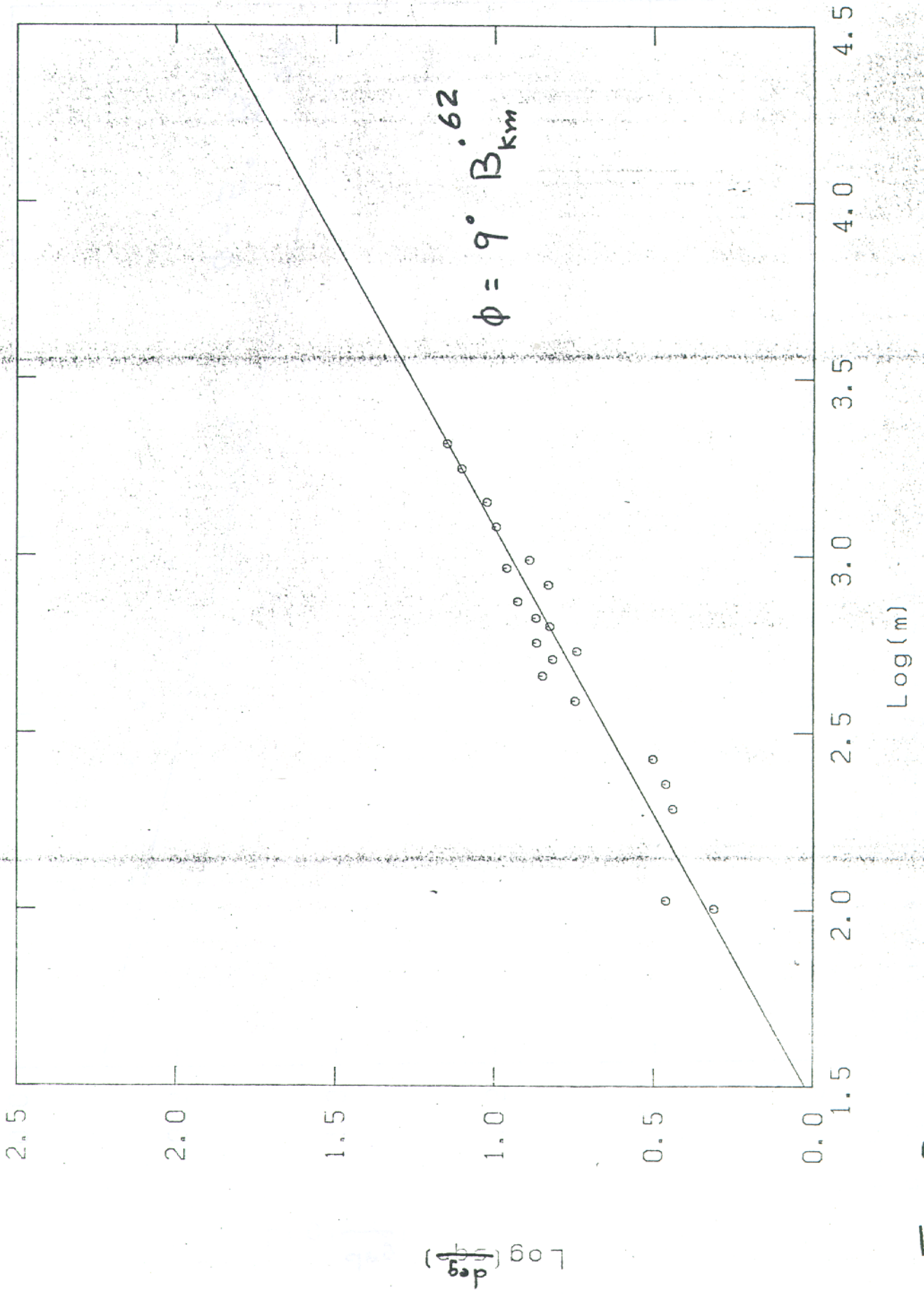


Fig. 2

p012a1; cal:none; alt sig2pt; rebin 0
tau = 16 min



$\phi = 5° \cdot B_{km}^{.26}$

Log(m)

$Log\left(\dfrac{deg}{}\right)$
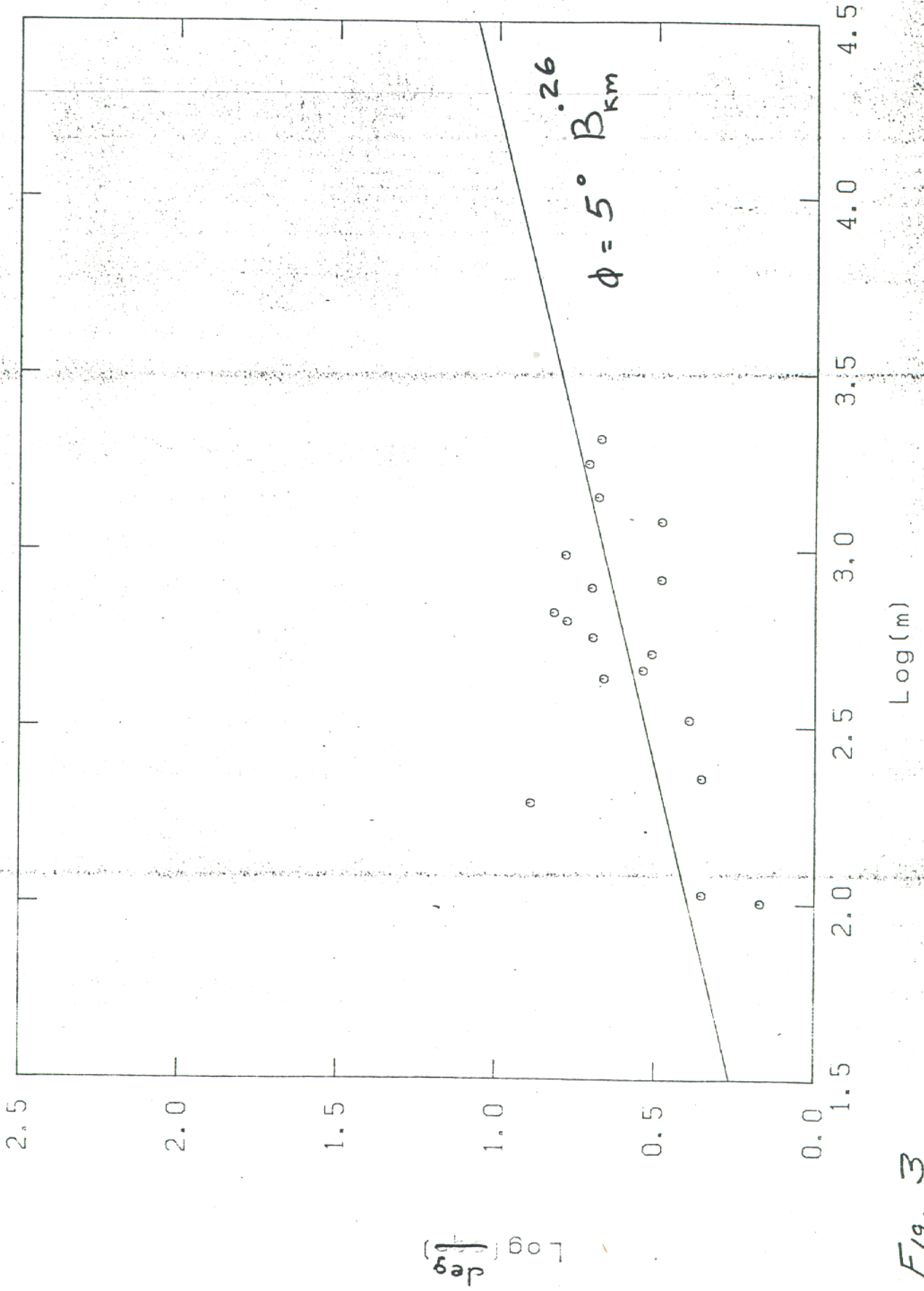
Fig. 3

$\sigma_B$  RMS about slope

x - uncalibrated
o - calibrated

$\Delta(\alpha,\delta) \sim 23°$

#

o·x
o·⟵———x
o·x
o·⟵———x

x·o

$\Delta(\alpha,\delta) \sim 6°$

#

o·⟵——x
x·———⟶o
o·⟵———x
o·⟵———x

0    10°    20    30    40    50°
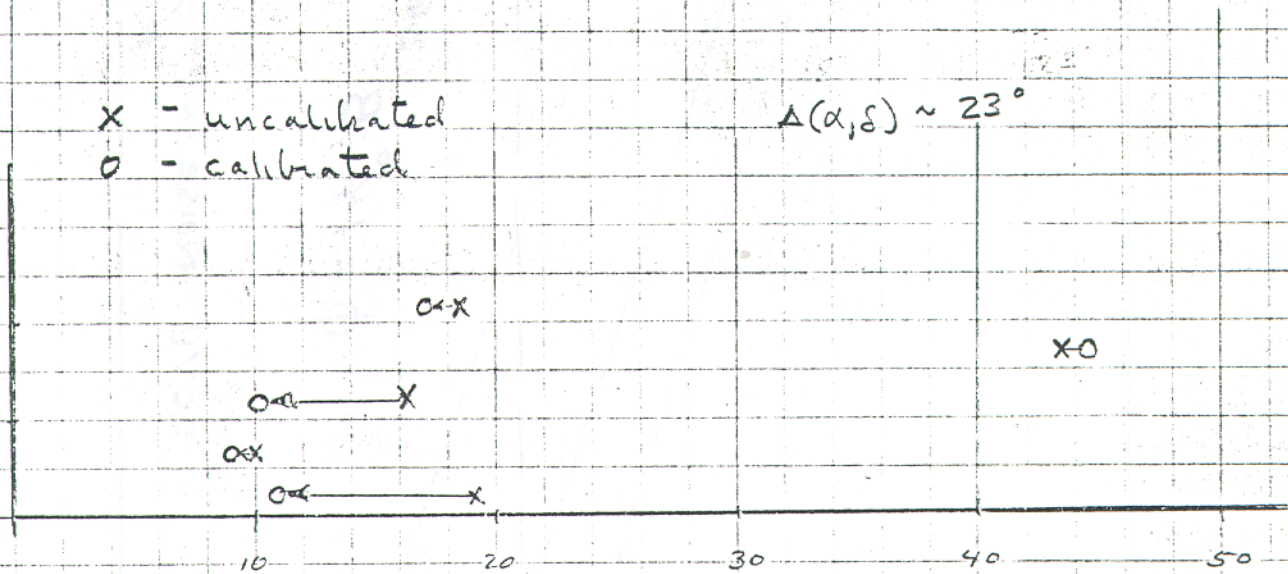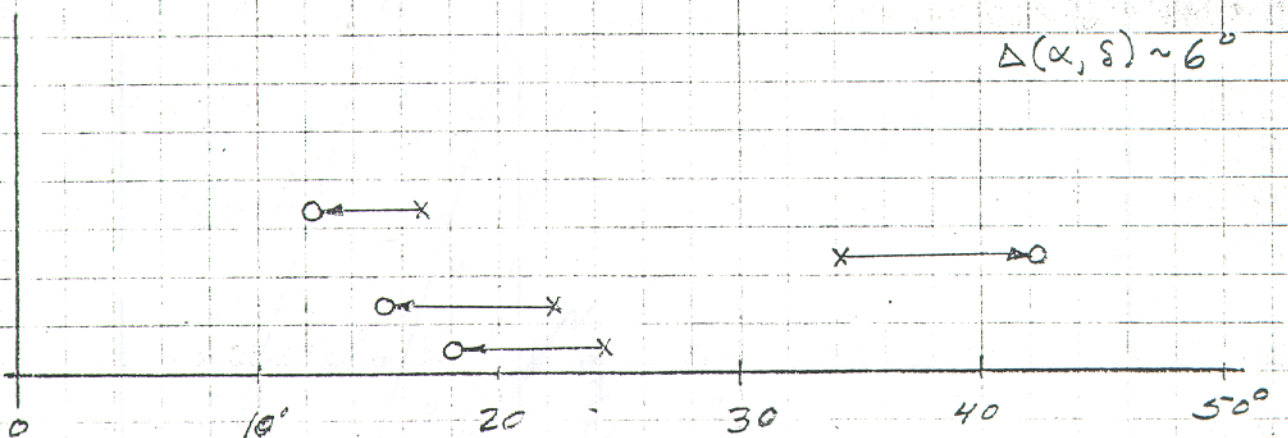
$\sigma_B$ (1km) (degrees @ 22.5 GHz)

$\tau_{ave} = 8\,min$

$\tau_{max} \sim 4\,hour$

$\tau_{CAL} = 16\,min$

| AVERAGE $\sigma_B$ (1km) $\Delta(\alpha,\delta)$ | | |
|---|---|---|
| | 6° | 23° |
| NO CAL | 25° | 21° |
| CAL | 22° | 18° |

Fig. 4

ave 18 run*sou; cal:none; sig2pt; rebin 2
tau = 16 min



14° @ 22GHz

$\phi = 14° B$ .36

RCVR Noise ~2°

Log(m)

Log(deg)
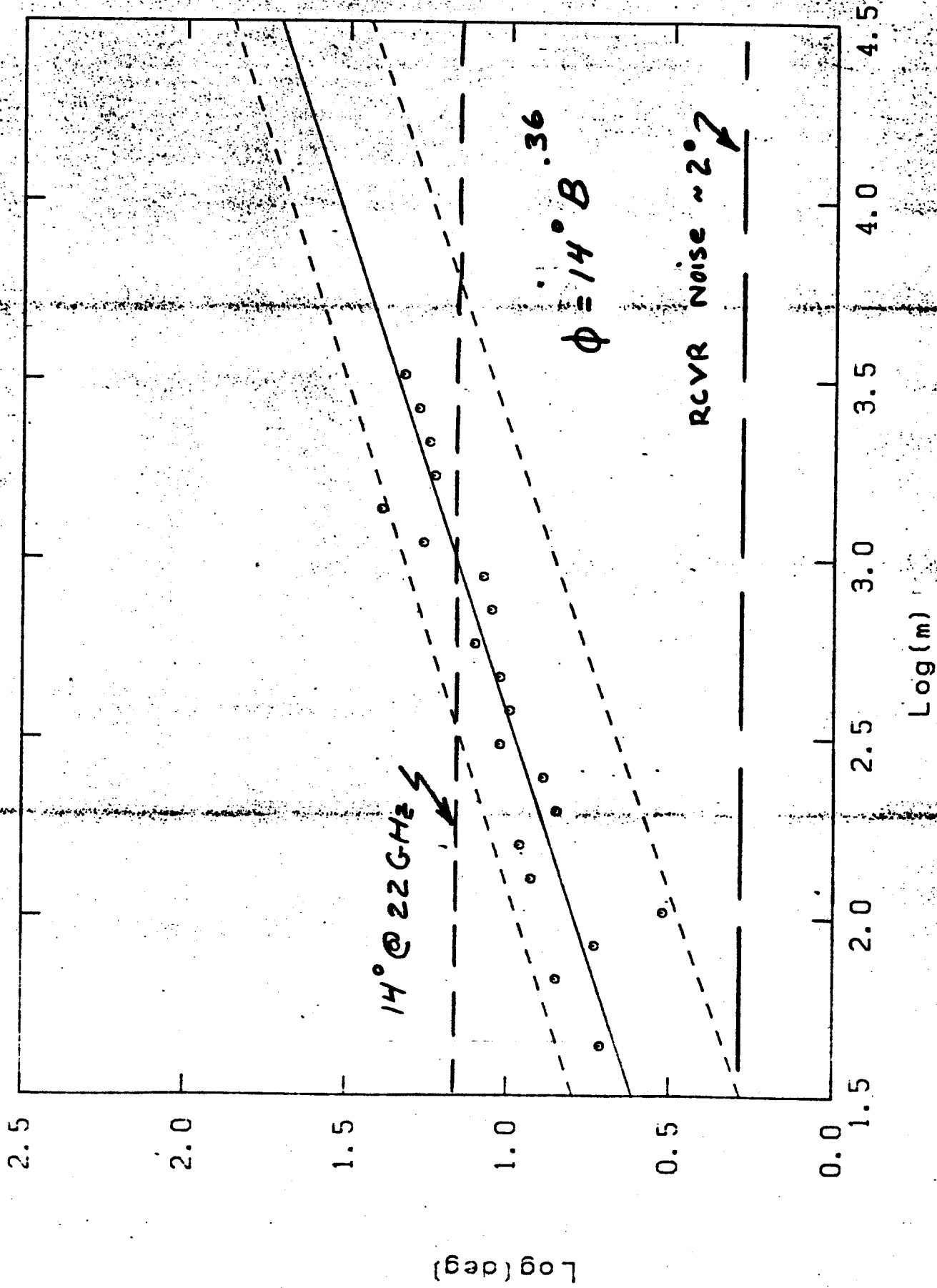
Fig. 5

ave.18 run*sou; cal:none; sig2pt; rebin 2
tau = 32 min

Log(m)

Log(deg)

$\phi = 17° B \cdot 41$
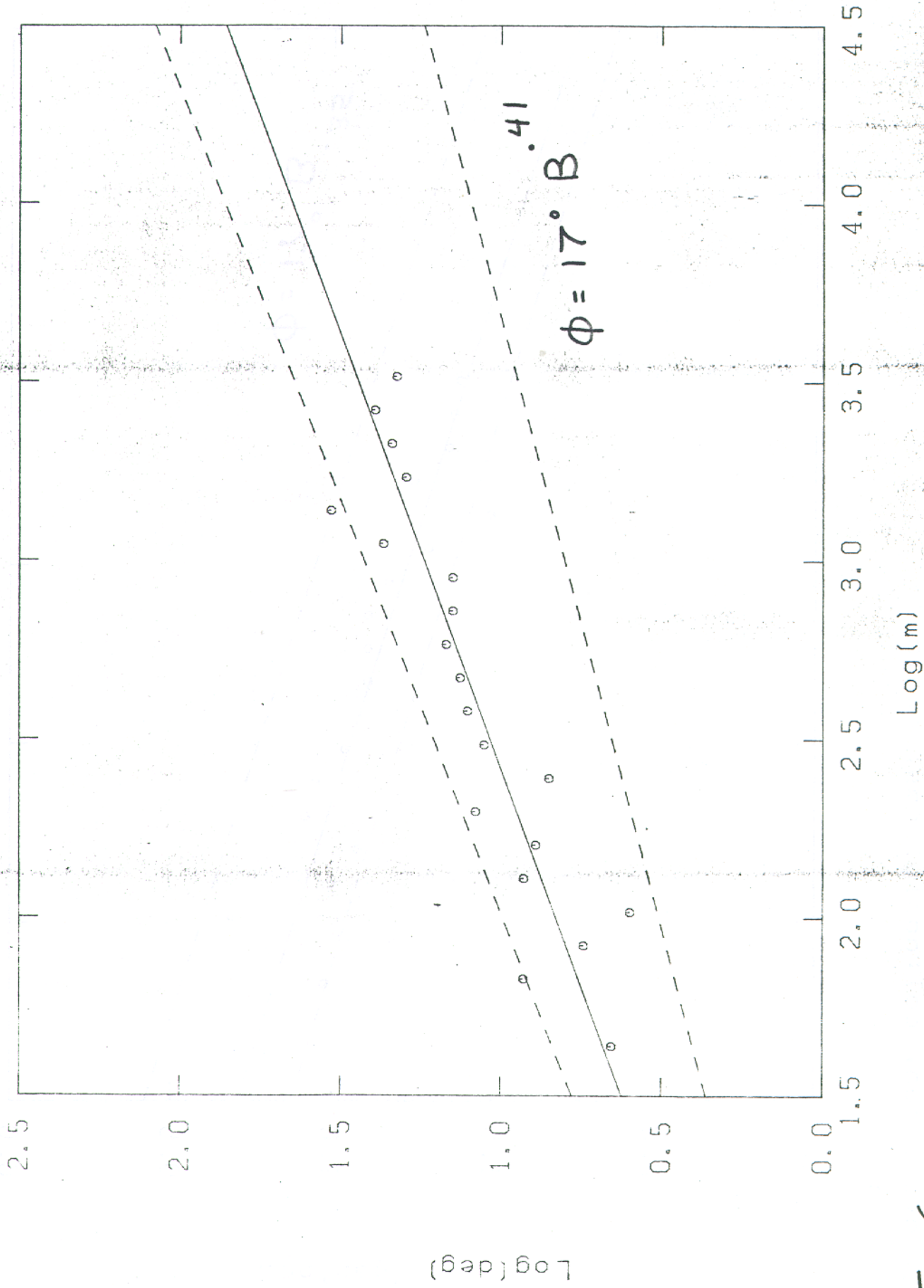
Fig. 6

ave 9 run; cal:apply; rms; rebin 2

RMS



$\phi = 17° \, \beta .35$

Log(m)

Log(deg)

Fig. 7

Fig 8

Fig. 9

Fig. 10



Fig. 11